CellPress

Trends in Biotechnology

Review

Advances in the Fabrication of Biomaterials for Gradient Tissue Engineering

Chunching Li,[1,2,3,7] Liliang Ouyang,[1,2,3,4,7,@] James P.K. Armstrong,[1,2,3,5,*,@] and Molly M. Stevens[1,2,3,6,*,@]

Natural tissues and organs exhibit an array of spatial gradients, from the polarized neural tube during embryonic development to the osteochondral interface present at articulating joints. The strong structure–function relationships in these heterogeneous tissues have sparked intensive research into the development of methods that can replicate physiological gradients in engineered tissues. In this Review, we consider different gradients present in natural tissues and discuss their critical importance in functional tissue engineering. Using this basis, we consolidate the existing fabrication methods into four categories: additive manufacturing, component redistribution, controlled phase changes, and postmodification. We have illustrated this with recent examples, highlighted prominent trends in the field, and outlined a set of criteria and perspectives for gradient fabrication.

Highlights

There has been a recent surge in the number of tissue-engineering protocols that use gradient biomaterials to replicate key developmental processes or functional roles.

Recent advances in additive manufacturing (e.g., 3D bioprinting, microfluidics) have led to increased structural complexity in bottom-up gradient biomaterial fabrication.

A growing number of reports are seeking to use applied forces that redistribute components of homogeneous systems to fabricate biomaterials with well-integrated gradients.

A small number of recent studies have fabricated gradient biomaterials by controlling the temperature or light exposure during hydrogel crosslinking.

Recent reports have demonstrated the fabrication of gradient biomaterials by postmodifying precast hydrogels or solid scaffolds using mechanisms based on temperature, light, or diffusion.

Gradients in Biology

Gradients are continuous transitions in the magnitude of a property along an axis and are a pervasive feature of biology, with conserved functional roles in tissue development and physiology. Here, we consider five classes of gradients that are widely found in natural tissues and tissue interfaces. *Cellular gradients* involve transitions in the density of one or more cell types; for example, **osteochondral tissue** (see Glossary) exhibits depth-dependent differences from the articulating surface to the underlying bone, with graded densities of **chondrocytes**, **hypertrophic chondrocytes**, and **osteoblasts** [1–3]. *Compositional gradients* are transitions in extracellular matrix (ECM) components; for example, mineral gradients are found in the dentin of human teeth [4], while collagen, proteoglycan, and hydration gradients are present throughout **articular cartilage** [5]. *Architectural gradients* are transitions in the organization of tissue components, such as the changes in porosity present in **cortical bone** [6] or the differences in fiber orientation across cardiac tissue [7]. Changes in tissue composition and architecture give rise to *mechanical gradients*, including transitions in compressive, tensile, and shear properties. Mechanical gradients are commonly found at load-bearing musculoskeletal interfaces, such as **entheses**, where they play an important role in the transmission of applied stresses [8].

Tissue gradients are established during development and maturation, processes that are guided by spatial variance in biochemical and biophysical cues [9]. In particular, *morphogen gradients* can arise through point-source diffusion or more complex intermediary mechanisms involving matrix components or extracellular vesicles [10]. These morphogen gradients generate cellular, compositional, architectural, and mechanical gradients by spatially regulating cell proliferation, migration, and differentiation [11]. For example, osteochondral tissue is derived from gradients of morphogens, such as Indian hedgehog, parathyroid hormone–related protein, and different bone morphogenetic proteins (BMPs) [12]. This directs the differentiation of an initially homogeneous pool of **osteochondroprogenitors** into a gradient of mature cells comprising chondrocytes, hypertrophic chondrocytes, and osteoblasts. These different cell populations

[1]Department of Materials, Imperial College London, Prince Consort Road, London, SW7 2AZ, UK
[2]Department of Bioengineering, Imperial College London, Prince Consort Road, London, SW7 2AZ, UK
[3]Institute of Biomedical Engineering, Imperial College London, Prince Consort Road, London, SW7 2AZ, UK
[4]Website (https://www.linkedin.com/in/liliang-ouyang-85724369).
[5]Website (www.jamespaularmstrong.co.uk).
[6]Website (www.stevensgroup.org).
[7]These authors contributed equally to this work.

 https://doi.org/10.1016/j.tibtech.2020.06.005

secrete distinct ECM components that provide the tissue with gradient mechanical properties to support the load-bearing function of osteochondral tissue [13]. This Review provides a comprehensive overview of recent approaches to forming gradient biomaterials for tissue engineering.

*Correspondence:
james.armstrong@imperial.ac.uk
(J.P.K. Armstrong) and
m.stevens@imperial.ac.uk
(M.M. Stevens).
@Twitter: @liliangouyang (L. Ouyang),
@jrmstrng (J.P.K. Armstrong), and
@ukrmp_smart (M.M. Stevens).

Engineering Gradients *In Vitro*

These various gradients are often overlooked during *in vitro* tissue engineering. This omission is surprising, given the importance of gradients to physiological function and the objective of tissue engineering: to replicate native tissue structures for *in vitro* modeling or *in vivo* tissue replacement [14]. Although homogeneous tissue constructs can provide information pertaining to physiology or pathology, a lack of structural organization can mask or limit contributing factors or functional outputs. Similarly, while clinical benefit can be realized by using uniform tissue grafts, their simplicity can restrict graft integration and limit full functional restoration [15]. Accordingly, the development of new methods that enable more faithful re-creation of natural morphologies has emerged as a major focus of translational tissue engineering. While acknowledging that specialized culture systems can present soluble morphogen gradients via the cell media [16,17], this Review focuses on the fabrication of gradient biomaterials for tissue engineering. Past reviews have focused on specific tissue gradients [18,19], while others have discussed specific gradient fabrication methods, such as 3D printing [20], microfluidics [21], **electrospinning** [22], self-assembly [22], and phase separation [22]. In recent years, there have been a number of new methods and adapted approaches that have presented new opportunities for tissue engineering. Here, we discuss these recent developments as part of a broad and comprehensive overview of gradient biomaterial fabrication. We define four overarching strategies that can be used to form gradients: additive manufacturing, component redistribution, controlled phase changes, and postmodification (Figure 1, Key Figure). We discuss key methods in each of these categories and explore their rationales, mechanisms, benefits, and limitations. Finally, we outline a set of key criteria for those seeking to develop new fabrication methods for gradient tissue engineering.

Additive Manufacturing

An early additive manufacturing approach was the use of adhesives to bind two or more solid biomaterial layers. For instance, cellularized osteochondral scaffolds have been prepared by using a small amount of solvent glue to bind different polymeric scaffolds [23]. More recently, glues such as alginate-boronic acid have been developed to bind precast hydrogels, such as agarose, acrylamide, and chitosan-catechol [24]. In these cases, however, the attractive interactions within each material layer are generally stronger than those bridging the interface, a situation that can result in delamination between the stacked layers. Thus, more recent work has focused on methods that can generate material layers without requiring an intermediary adhesive (Figure 1A). For example, the addition of a liquid precursor to a mold followed by partial crosslinking can be repeated to build sequentially layered structures. This approach has recently been used by Guo and coworkers to create compositional gradients of mineralizing peptide in stacked silk fibroin hydrogels (Figure 2A) [25] and by Ko and coworkers to form compositional gradients in gelatin methacryloyl (GelMA) hydrogels [26]. Meanwhile, Parisi and coworkers showed that slurries of collagen and hydroxyapatite (HAP) at varying ratios could be sequentially stacked and collectively lyophilized to form integrated osteochondral scaffolds with compositional and mechanical gradients [27]. In 2016, Levingstone and coworkers reported an 'iterative layering freeze-drying' approach using multiple steps of **lyophilization**, crosslinking, and rehydration to create trilayer osteochondral scaffolds [28]. Meanwhile, an ingenious method reported by Wei and coworkers in 2017 showed that precast hydrogel modules could be assembled into gradient biomaterials using a Schiff base 'self-healing' mechanism [29]. An inherent limitation of all of these methods is that the material is composed of discrete layers (a stepped transition) rather than a smooth profile (a continuous gradient).

Greater structural complexity can be achieved using 3D printing, in which a digital model is replicated as a solid or porous 3D object using controlled fluid deposition [20,30,31]. Mechanically graded structures can be assembled by varying the ink composition or the print design. In 2017, Trachtenberg and coworkers reported a gradient distribution of HAP nanoparticles in a 3D printed composite scaffold [32], while in 2019, Bittner and coworkers described the use of 3D fiber deposition to create poly(ε-caprolactone) (PCL)-based scaffolds with architectural gradients (porosity) and compositional gradients [33]. Meanwhile, 3D printed scaffolds with pore size gradients were reported by Di Luca and coworkers in 2016 and used to spatially modulate the **chondrogenic** differentiation [34] or **osteogenic** differentiation [35] of human **mesenchymal stem cells** (hMSCs). In 2020, Smith and coworkers also described the use of extrusion-based 3D printing to generate compositional and architectural (porosity) gradients to direct stem cell differentiation down the osteogenic lineage. The authors observed that increased concentration of β-tricalcium phosphate and higher scaffold porosity induced a more mature osteogenic phenotype [36]. Other groups have also recently used 3D printed scaffolds with graded pores as sacrificial templates [37,38]. Although the majority of studies have reported the fabrication of vertical gradients, recent improvements in instrumentation have enabled the effective printing of lateral gradients. In 2019, Diaz-Gomez and coworkers described the use of multimaterial segmented fiber printing to generate lateral gradients in composition and porosity [39], while in 2020, Giachini and coworkers used a feedback loop to synchronize extrusion and deposition to print multidirectional lateral gradients in composition, architecture, and stiffness [40].

These examples all focus on the fabrication of *acellular* gradient scaffolds, which can be seeded with cells after printing. An alternative strategy is 3D **bioprinting**, in which cells can be printed in either biomaterial-free [41,42] or biomaterial-based **bioinks** [43,44]. High-energy processes, such as selective laser sintering, are poorly suited for printing viable cells, but extrusion printing, inkjet printing, and lithography-based printing can all be used to fabricate structures with high cell viability [45]. The inclusion of cells within the bioink presents the opportunity to directly fabricate defined cellular gradients. In 2017, Graham and coworkers generated different high-resolution tissue architectures by printing cell-laden droplets, including cellular gradients of osteoblasts and chondrocytes [46]. Meanwhile, in 2015, Hardin and coworkers demonstrated the use of microfluidic printheads to achieve controlled mixing of different inks before deposition, which allowed continuous gradients to be formed in the extruded fibers [47]. In 2019, Idaszek and coworkers used this principle to mix doped alginate-based solutions for the bioprinting of graded cell-laden constructs to mimic the ECM organization of native cartilage (Figure 2B) [48]. In 2017, Liu and coworkers reported the use of a microfluidic mixing printhead with multiple input channels to controllably deposit up to seven inks and generate tunable structures with various cellular and compositional gradients [49]. The major benefit of 3D printing is the precise spatial control, which enables the generation of multiple gradients within tunable material architectures. However, only a small class of materials has the required characteristics needed for 3D printing, and only a subset of these materials are capable of supporting viable cell populations [50,51].

Other continuous deposition processes can also be used to fabricate gradient materials. For example, commercially available 'gradient makers' continually feed solutions from different reservoirs into a single joined outlet, with the mixed liquid then deposited and cast in a mold. By controlling the relative flow rates during the casting process, different gradients can be produced. In 2018, Zhu and coworkers used a gradient maker to generate mechanically graded tissue constructs by casting a chondrocyte-laden hydrogel precursor solution with two different biopolymer concentrations [52]. Controlled fluid deposition can also be achieved through the use of bespoke microfluidic platforms [53]. In 2017, Orsi and coworkers reported the fabrication of polyacrylamide hydrogels with mechanical gradients using a chamber integrated with multiple microfluidic

Glossary

Articular cartilage: load-bearing collagenous tissue present at the end of long bones.
Bioinks: the fluids, typically containing viable cells, deposited during bioprinting.
Bioprinting: the use of computer-aided transfer processes for the patterning and assembly of living and nonliving materials with a defined 2D or 3D architecture.
Cortical bone: dense mineralized tissue found predominantly at the surface of long bones and flat bones.
Chondrocytes: mononucleate, rounded cells of mesenchymal origin that are responsible for the formation and remodeling of cartilage tissue.
Chondrogenic: relating to the formation of cartilage.
Electrospinning: a processing method that uses electric fields to generate fibrous scaffolds from polymer solutions.
Entheses: interfacial tissue where bone forms a connection to a tendon, ligament, fascia, or capsule.
Glioma cell: a cancer cell type thought to arise from nonmalignant glial cells.
Hypertrophic chondrocytes: nonproliferative swollen chondrocytes that direct mineralization and vascularization during endochondral bone formation.
Lyophilization: the sublimation of ice from frozen materials at reduced pressure; synonym for 'freeze-drying.'
Mesenchymal stem cells: multipotent cells that give rise to cells of chondrogenic, osteogenic, and adipogenic lineage.
Neural tube: the embryonic precursor to the central nervous system.
Osteoblasts: mononucleate, cuboid cells of mesenchymal origin that are responsible for the formation of bone tissue.
Osteochondral tissue: interfacial tissue comprising subchondral bone and articular cartilage.
Osteochondroprogenitors: progenitor cells of mesenchymal origin that give rise to osteoblasts or chondrocytes.
Osteogenic: relating to the formation of bone.

Key Figure

Four Categories of Gradient Fabrication.

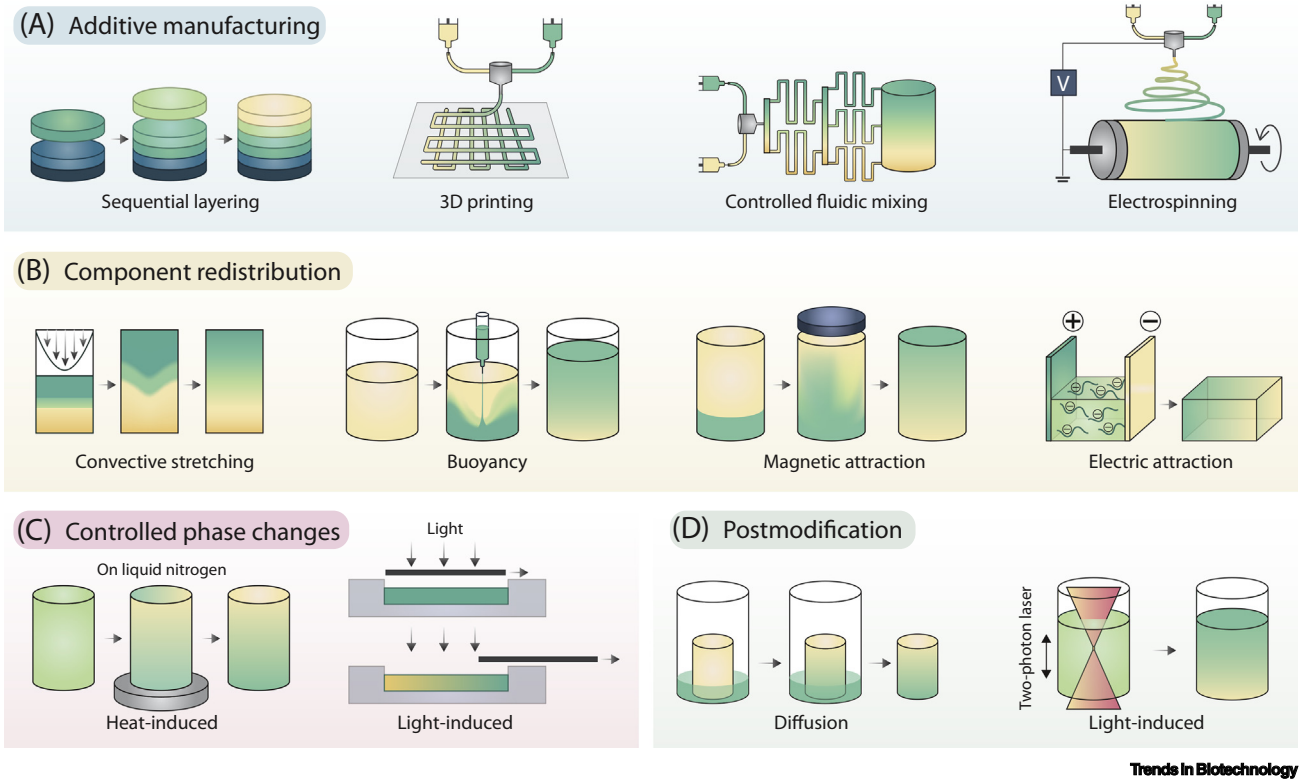

Figure 1. (A) Additive manufacturing is an intuitive approach to gradient fabrication, with methods including sequential layering, 3D printing, controlled fluidic mixing, and electrospinning. (B) Component redistribution approaches produce gradients from an initially homogenous distribution by controlled demixing via convective stretching, buoyancy, magnetic fields, or electric fields. (C) Controlled phase changes can also result in the formation of gradients from homogeneous starting materials, typically using graded exposure to heat or light. (D) Postmodification involves the presentation of a gradient onto preformed materials, typically achieved by controlled component diffusion or photopatterning.

inlets [54]. In 2019, Hubka and coworkers used a similar principle to form gradients of perlecan domain I across hyaluronic acid (HA)-based hydrogels. The perlecan domain was then used to sequester and release fibroblast growth factor, a morphogen gradient that was used to direct cell migration [55]. Two innovative approaches were reported in 2019, both using microfluidic mixing and deposition. Xin and coworkers used microfluidic droplet generators to produce poly (ethylene glycol) (PEG)-based microgels, which were deposited into syringes and used to form microporous annealed particle hydrogels. By adjusting the input polymer components during the microdroplet fabrication, the authors produced hydrogels with gradients in microgel composition that were preserved after annealing [56]. Meanwhile, Costantini and coworkers used an adjustable, valve-based, flow-focusing junction to generate foams with tunable bubble size. This method was used to fabricate gelatin and gelatin/HAP scaffolds with architectural gradients in pore size (80–800 μm) (Figure 2C) [57].

By controlling the fluid deposition process, electrospinning can also be used to fabricate gradient materials. Typically, reservoirs loaded with different polymer solutions are either sequentially

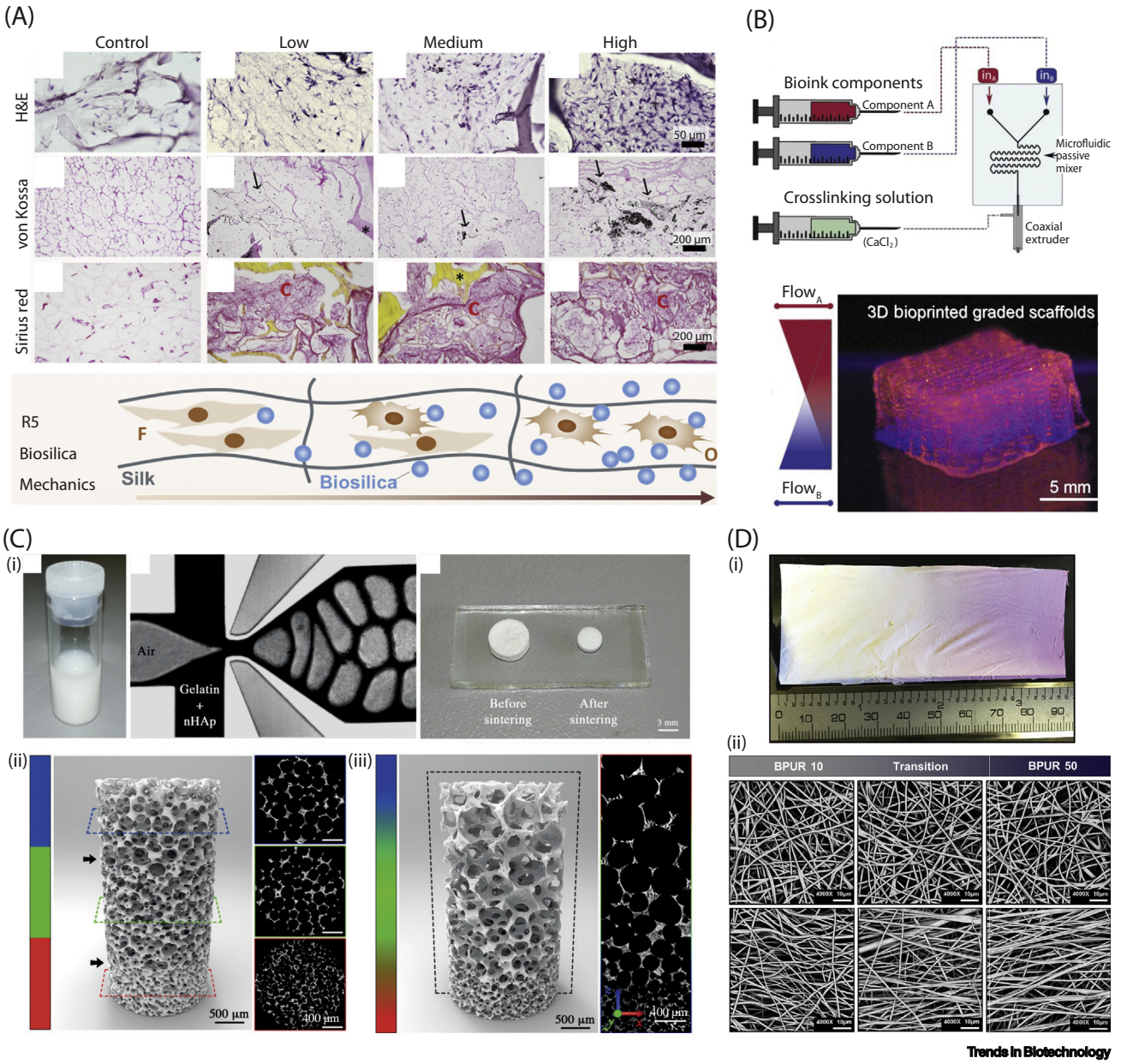

Figure 2. Additive Manufacturing of Gradient Biomaterials. (A) Osteochondral tissue engineered using mesenchymal stem cells seeded on a sequentially layered scaffold with low, medium, and high loading of a mineralizing peptide (R5). Images showing hematoxylin and eosin (H&E), von Kossa, and Sirius red staining of histological sections. Reproduced, with permission, from [25]. (B) 3D printing scaffolds with compositional gradients using a microfluidic printing head to controllably mix solution components prior to extrusion. Reproduced, with permission, from [48]. (C) (i) Fabrication of scaffolds with architectural gradients in porosity using a valve-based, flow-focusing microfluidic device to create gelatin and nano-hydroxyapatite (nHAP) composite foams with tunable bubble size. 3D reconstructions using micro–computed tomography of the resulting (ii) multilayered and (iii) graded porous materials. Reproduced, with permission, from [57]. (D) (i) Electrospun scaffolds with compositional gradients fabricated from two different biodegradable poly(urethane urea) (BPUR) fibers. (ii) Scanning electron micrographs of different regions across random and aligned gradient scaffolds. Reproduced, with permission, from [60].

deposited or mixed at varying ratios and then controllably electrospun onto a moving collector [58,59]. In 2017, Kishan and coworkers reported the use of sequential electrospinning to generate meshes with compositional gradients of two different poly(ester urethane urea) fibers and

architectural gradients in fiber alignment (Figure 2D) [60]. A similar approach was described by Khoo and coworkers in 2019, in which trilayer gelatin meshes were fabricated with architectural gradients in fiber diameter (227–679 nm) and pore size (1.14–4.93 μm^2) [61]. In 2019, Horner and coworkers reported an example of sequential core-shell electrospinning in which the ratio between the PEG core and the PCL shell was varied during the deposition process. This method produced scaffolds with architectural gradients in fiber shell thickness and mechanical gradients in compressive modulus (3–19 kPa), thus allowing the effect of mechanical gradients on hMSC differentiation to be studied in scaffolds with homogeneous composition and topography [62].

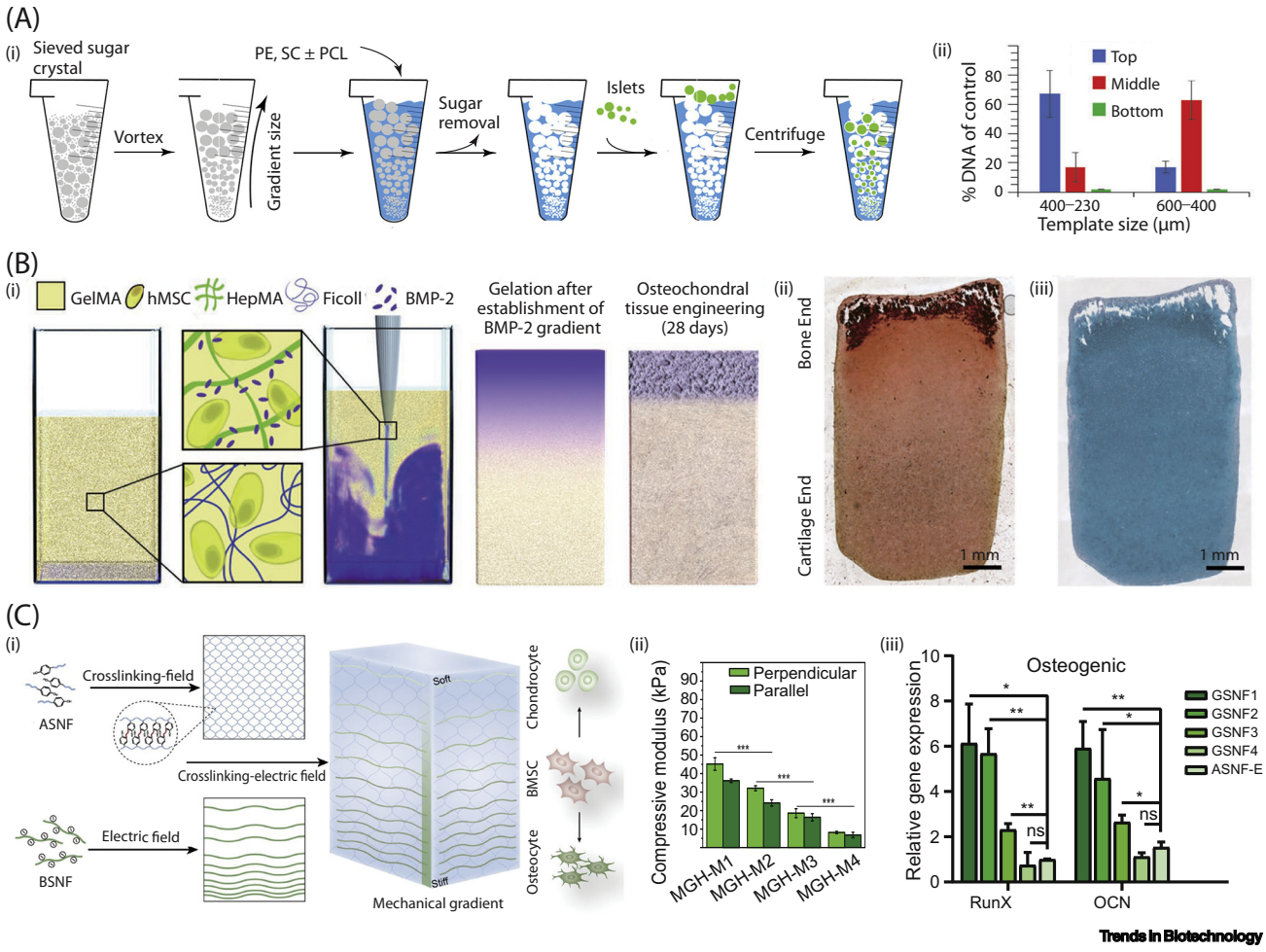

Figure 3. Component Redistribution Approaches for Gradient Biomaterial Fabrication. (A) (i) Scaffolds with architectural gradients in pore size were templated by gradients of sugar particles (gray) formed via granular convection. After adding and crosslinking a polymer precursor solution (blue) comprising pentaerythritol (PE), sebacoyl chloride (SC), and poly(ε-caprolactone) diol (PCL), the templates were dissolved, and human pancreatic islets (green) were seeded in the resulting pores. (ii) The number of human islets retained throughout the scaffold with the different template size ranges. Reproduced, with permission, from [63]. (B) (i) Osteochondral tissue, engineered using of human mesenchymal stem cell (hMSC)-laden gelatin methacryloyl (GelMA) hydrogels, with buoyancy used to form a morphogen gradient of bone morphogenetic protein 2 (BMP-2) complexed with heparin methacrylate (HepMA). The resulting tissue was stained with (ii) Alizarin Red S to reveal the presence of a mineralized cap and (iii) Alcian blue staining to visualize the distribution of sulfated glycosaminoglycans. Reproduced, with permission, from [66]. (C) (i) Cell-supportive gradient biomaterials generated by the migration of β-sheet rich silk fibroin nanofibers (BSNF) through hydrogel precursors under an applied electric field. (ii) The gradient, silk-laden GelMA hydrogels were equally divided into four regions (termed MGH-M1, MGH-M2, MGH-M3, MGH-M4). Compression testing performed on these four regions revealed the presence of a mechanical gradient in compressive modulus. (iii) Gene expression of Runt-related transcription factor 2 (RunX) and osteocalcin (OCN) in mesenchymal stem cells after 28 days of osteogenic differentiation in amorphous silk fibroin nanofiber (ASNF) hydrogels and in different regions of gradient silk fibroin nanofiber (GSNF) hydrogels. *$P \leq 0.05$, **$P \leq 0.001$. Abbreviation: BMSC, bone mesenchymal stem cell. Reproduced, with permission, from [70].

Overall, electrospinning, microfluidics, and gradient makers have enabled the rapid fabrication of continuously graded biomaterials; however, these methods are generally restricted to simple, unidirectional gradients.

Component Redistribution

The previous examples all involve the direct deposition of materials at different spatial coordinates along the gradient axis. An alternative approach is to start with a homogeneous system and use an applied force to redistribute components into a gradient (Figure 1B). In 2020, Forget and coworkers reported that vortex mixing could be used to redistribute dried sucrose microparticles by size, based on the principle of granular convection. The sucrose microparticles were used as porogens to template the formation of polyester–ether scaffolds with architectural gradients in pore size (Figure 3A) [63]. A more common strategy is the redistribution of fluid components through the use of controlled demixing processes. An early example of this approach is the use of centrifugal forces to fabricate collagen–glycosaminoglycan scaffolds with architectural gradients in pore size [64] and crosslinked PCL fibril scaffolds with architectural gradients (porosity) and morphogen gradients [65]. More recently, it has been shown that spontaneous demixing can be used for gradient biomaterial fabrication. Li and coworkers reported in 2019 that density differences between mixed fluid phases could lead to predictable demixing and the formation of materials bearing tunable compositional, mechanical, and morphogen gradients [66]. This method was used to present a gradient of BMP-2 across a GelMA hydrogel laden with hMSCs in order to locally stimulate osteogenic differentiation and mineralization during osteochondral tissue engineering (Figure 3B). While this method can support multiple gradient applications, it requires a density difference and is restricted to a single gradient in one construct. An alternative approach is to use microfluidic devices to create controlled flow shear stretching and diffusion spreading, which was used in early work to fabricate compositional gradients [67]. More recently, thermally induced convective flow has been used to form biomaterials bearing compositional gradients without the use of microfluidics. Canadas and coworkers reported in 2018 that composite gradient hydrogels could be prepared by mixing a cooled solution of GelMA and gellan gum to a similar solution that had been prewarmed and doped with HAP. A 10°C temperature difference between the two fluids was sufficient to generate compositional gradients in HAP, which were immobilized by gelation and used for osteochondral tissue engineering [17].

Convection-, gravity-, or buoyancy-based approaches exploit physical material differences (e.g., temperature, size, density), which enable gradients to be formed without needing to modify any of the components. Other approaches have sought to modify individual tissue-engineering components so that they can be selectively manipulated using applied fields. In 2020, Zwi-Dantsis and coworkers used antibody-conjugated superparamagnetic iron oxide nanoparticles (SPIONs) to magnetize cardiomyocytes derived from human induced pluripotent stem cells. An external magnetic field was then used to generate different cellular gradients of cardiomyocytes, encapsulated in collagen hydrogels for cardiac tissue engineering [68]. A similar approach was reported by Li and coworkers in 2018, who showed that BMP-2 could be loaded into heparin-modified SPIONs and selectively redistributed into a gradient using an external magnetic field [69]. These morphogen gradients were formed across agarose hydrogels laden with hMSCs to form integrated osteochondral tissue constructs. Meanwhile, in 2020, Xu and coworkers reported the formation of biomaterials with compositional and mechanical gradients using electric field migration. In this work, β-sheet rich silk nanofibers moved to the anode of an applied electric field, with the migration kinetics tuned to the gelation rate of the surrounding polymer (GelMA, *N*-isopropylacrylamide, or amorphous silk nanofiber solution) (Figure 3C) [70].

Controlled Phase Changes

The examples discussed thus far have all involved the controlled distribution of bulk materials or material components. An alternative approach is to form gradients through spatially controlled crosslinking, a particularly attractive option for fabricating materials with architectural or mechanical gradients (Figure 1C). Graded light exposure has been widely used to vary the degree of crosslinking across different hydrogels. Major and coworkers recently used gradient photomasks to produce GelMA hydrogels with continuous mechanical gradients in stiffness (5–38 kPa). The authors showed that adipose-derived stem cells encapsulated in low-stiffness regions exhibited an increased cellular and nuclear volume and enhanced nuclear localization of mechanosensitive proteins (Figure 4A) [71]. Meanwhile, Dou and coworkers used sliding photomasks to fabricate polyacrylamide hydrogels with longitudinal mechanical gradients in stiffness (1–40 kPa) capable of guiding **glioma cell** migration [72].

An alternative, temperature-based approach was demonstrated by Kim and coworkers in 2015, who used a unidirectional freezing process to create transitions in the crystallinity of poly(vinyl alcohol) (PVA) hydrogels. This was possible due to the unusual hydrogelation mechanism of PVA, in which ice crystals induce the formation of localized polymer crystallites that facilitate network

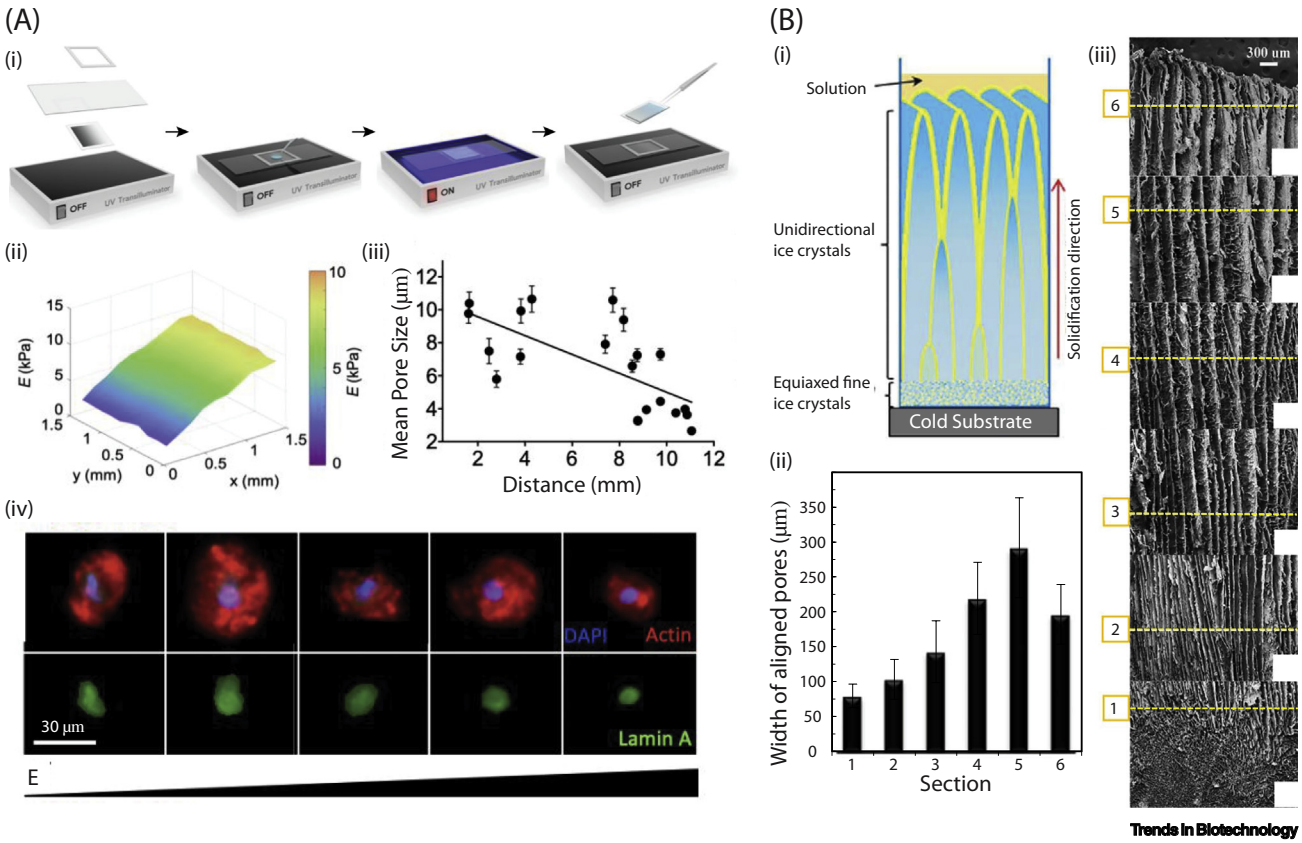

Figure 4. Controlled Phase Changes for Gradient Biomaterial Fabrication. (A) (i) Fabrication of graded photocrosslinkable biomaterials using gradient photomasks. (ii) Optical coherence elastography and (iii) pore size measurements were performed on the resulting materials to measure mechanical gradients (stiffness) and architectural gradients (porosity), respectively. (iv) Morphology of adipose-derived stem cells encapsulated in the gradient GelMA hydrogels. Reproduced, with permission, from [71]. (B) (i) Scaffolds fabricated by ice-templating starch and poly(vinyl alcohol) (PVA) composite hydrogels under thermal gradients. (ii) The resulting composite materials exhibited architectural gradients in pore width, as determined by image analysis of (iii) scanning electron micrographs. The section numbers in (ii) refer to measurements taken from regions denoted in (iii). Reproduced, with permission, from [74].

crosslinking [73]. This methodology was later extended to semi-interpenetrating networks of PVA and HA, which widened the stiffness range to 20–200 kPa. In 2018, Mirab and coworkers used a similar approach to fabricate lyophilized starch/PVA scaffolds with architectural gradients in pore width (80–292 μm) (Figure 4B). A citric acid crosslinker, osteoblasts, cellulose, and HAP were incorporated into the scaffolds, which were then used for bone tissue engineering [74]. Similar methods have been used to create ice fronts that move through a liquid precursor, initiate ice crystallization, and generate materials with spatial differences in material porosity. This ice-templating approach was used by Bai and coworkers in 2015 to fabricate HAP scaffolds with architectural gradients in channel width (4.5–8.1 μm) [75]. In 2017, Pawelec and coworkers used a similar method to template collagen-based hydrogels with architectural gradients in pore size (80–600 μm), a permeability range that was shown to affect the migration of seeded osteoblast-like cells [76].

Postmodification

The previous examples have involved the formation of gradients during the fabrication process; a counterstrategy is the postmodification of preformed solids or hydrogels (Figure 1D). This approach has been most readily used to produce materials with compositional gradients. Early examples involved the gradual introduction of solution components to scaffolds by dip-coating [77] or controlled immersion [78]. A more recent trend has been the use of controlled diffusion to generate uneven distributions of molecular components. In 2015, Gunnewiek and coworkers used molecular diffusion to create longitudinal and radial gradients of immobilized proteins across porous PCL scaffolds [79]. In 2018, Xu and coworkers reported that diffusion could be used to form gradients of a bifunctional crosslinker across pre-cast Matrigel. The crosslinker was immobilized to the Matrigel, uncaged by light, and used as a reactive base to bind semaphorin 3A (Sema3A), which was also introduced via a diffusion gradient (Figure 5A). Depth-dependent gradients of Sema3A are believed to direct radial migration of neurons during cortical development, and the authors observed evidence of enhanced cortical regeneration after implanting the Sema3A Matrigel gradient into a rat model of traumatic brain injury [80]. Strategies based on controlled adsorption or diffusion are relatively simple and accessible; however, they often require an optimized set of parameters that limit the rate of a molecular process without impeding it entirely.

Postmodification can also be performed using spatially modulated light exposure [81]. In 2016, Tong and coworkers reported the use of sliding photomasks to vary the photocrosslinking of norbornene-functionalized PEG hydrogels with cysteine-terminated RGD peptide. This method was applied to hydrogels that were already cast with a mechanical stiffness gradient [82]. Orthogonal compositional gradients were also reported by Vega and coworkers, who used sequential sliding photomasks to immobilize different peptides to norbornene-functionalized, HA-based hydrogels (Figure 5B) [83]. An alternative approach was demonstrated in a seminal paper by Mosiewicz and coworkers in 2013. The authors showed that laser-scanning lithography could be used to uncage enzymatic peptide substrates tethered to PEG-based hydrogels. The resulting enzymatic crosslinking enabled the presentation of gradients of covalently bound proteins, such as vascular endothelial growth factor [84]. The Shoichet group have developed similar methods, in which light was used to deprotect or uncage hydrogel-bound thiols that were used to subsequently bind bioactive peptides or proteins [85,86]. In 2018, they showed that HA-based hydrogels functionalized with nitrodibenzofuran-caged thiols could form exposed thiol gradients following repeated two-photon laser scanning. An intermediary click reaction between the uncaged thiol and maleimide-functionalized streptavidin produced gradients of biotinylated epidermal growth factor, which was shown to direct cancer cell invasion [86].

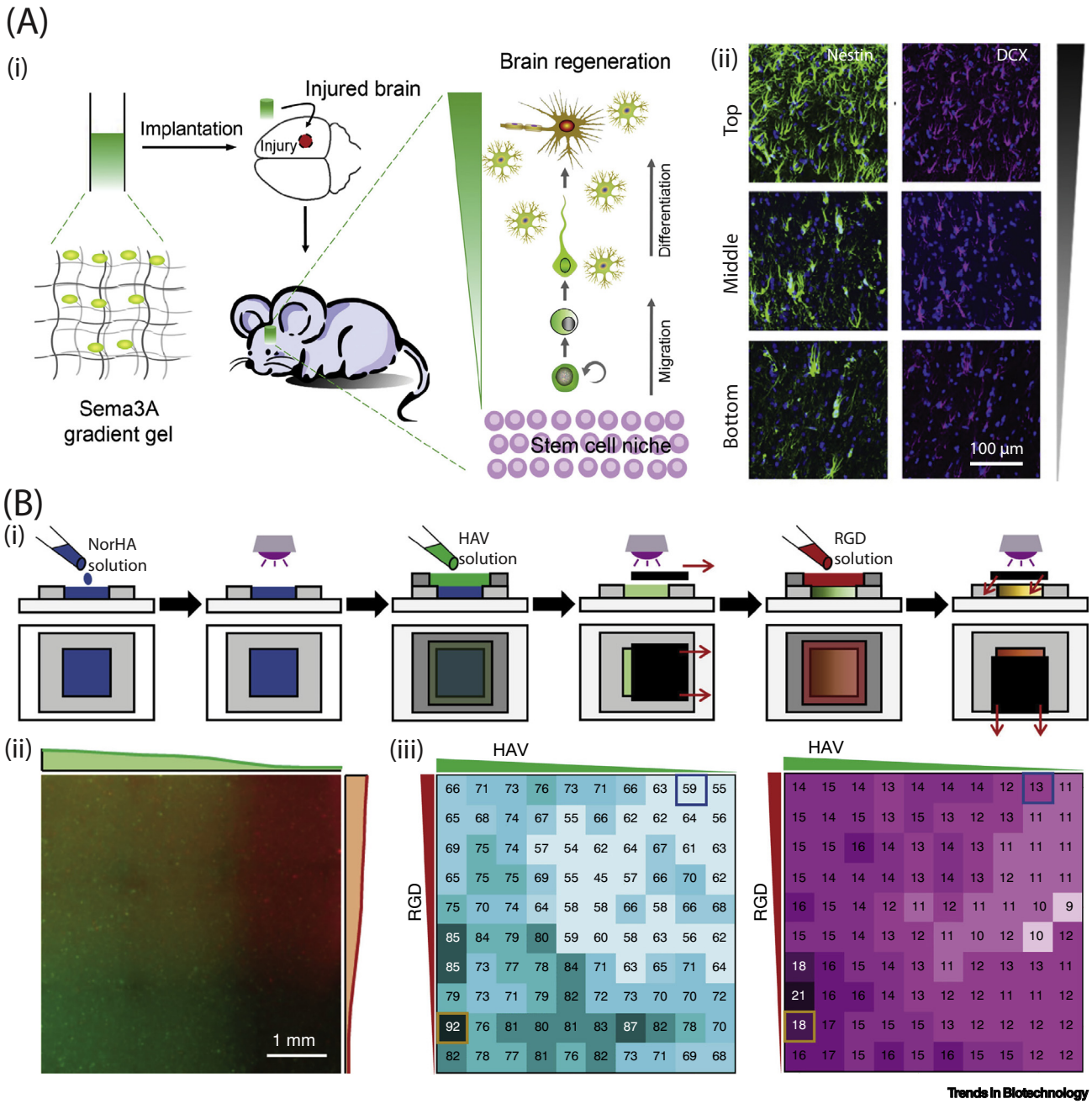

Figure 5. Postmodification to Form Gradient Biomaterials. (A) (i) Gradient biomaterials prepared by the sequential diffusion of a bifunctional crosslinker and semaphorin 3A (Sema3A) into a Matrigel hydrogel and used for *in vivo* implantation. (ii) Fluorescence images showing the distribution of Nestin^{+} (green) and doublecortin-positive (DCX^{+}; red) cells that had migrated into different regions of the gradient hydrogels. Reproduced, with permission, from [80]. (B) (i) Orthogonal gradients patterned into norbornene-functionalized hyaluronic acid (NorHA) hydrogels by sequential photocrosslinking of HAV and RGD peptides, with light exposure controlled using a sliding photomask. (ii) Fluorescence imaging of the orthogonal gradients with rhodamine-labeled RGD (red) and fluorescein-labeled HAV (green). (iii) The orthogonal gradients were shown to regulate the expression of Sox9 (blue) and the synthesis of aggrecan (purple). Values indicated are based on normalized intensity. Reproduced, with permission, from [83].

Table 1. Gradient Fabrication Strategies and Selected Examples

Additive manufacturing	Advantages	Disadvantages	Examples	Refs
Layering	• Rapid and simple protocol • No specialist equipment	• Restricted to stepped transitions • Risk of delamination	• Compositional • Mechanical	[23,25–28] [25,27]
3D printing	• Free-form control over the material architecture • Can form continuous gradients • Can form a range of gradients	• Requires printable materials • Requires specialist equipment and significant user expertise	• Cellular • Architectural • Mechanical • Compositional	[46] [33–40] [40] [32,33,36,40,47–49]
Fluid mixing	• Rapid and simple protocol • Can form continuous gradients • Can form a range of gradients	• Restricted to single gradients	• Compositional • Morphogen • Mechanical • Architectural	[52,55,56] [55] [54] [57]
Electrospinning	• Rapid and simple protocol • Can form continuous gradients • Can form a range of gradients	• Restricted to thin scaffolds • Challenging with live cells	• Compositional • Architectural • Mechanical	[60] [61,62] [62]
Component redistribution	**Advantages**	**Disadvantages**	**Examples**	**Refs**
Convection	• Rapid and simple protocol • Can form continuous gradients	• Requires certain geometry and convective conditions	• Compositional • Architectural	[17,63,67] [63]
Centrifugation	• Rapid and simple protocol • Can form continuous gradients	• Requires a density difference • Restricted to single gradients	• Compositional • Architectural • Morphogen	[65] [64] [65]
Buoyancy	• Rapid and simple protocol • Can form continuous gradients • Can form a range of gradients	• Requires a density difference • Restricted to single gradients	• Compositional • Mechanical • Morphogen	[66] [66] [66]
Magnetic fields	• Rapid and simple protocol • Can form continuous gradients	• Requires magnetic particles • Risk of particle cytotoxicity	• Cellular • Morphogen	[68] [69]
Electric fields	• Can form continuous gradients	• Requires field responsivity • Risk of electrical cytotoxicity	• Compositional • Mechanical	[70] [70]
Controlled phase changes	**Advantages**	**Disadvantages**	**Examples**	**Refs**
Heat-induced	• Rapid and simple protocol • Can form continuous gradients	• Requires thermoresponsivity at suitable temperatures	• Architectural • Mechanical	[74–76] [73]
Light-induced	• High resolution • Can form continuous gradients	• Requires photoresponsivity • Risk of cell damage from UV light or free radicals	• Mechanical	[71,72,83]
Postmodification	**Advantages**	**Disadvantages**	**Examples**	**Refs**
Dipping or filling	• Rapid and simple protocol • Can form continuous gradients	• Requires relatively rapid binding kinetics	• Compositional	[77,78]
Diffusion	• Simple protocol • Can form continuous gradients	• Requires optimized mass transport conditions • Slow fabrication process	• Compositional	[79,80]
Light-induced	• High resolution • Can form continuous gradients	• Requires photoresponsivity • Risk of cell damage from UV light or free radicals	• Compositional	[82–86]

General Criteria for Gradient Fabrication

The approaches discussed in this Review each have specific merits and limitations (Table 1). Taking these into consideration, several principles should be applied when designing a fabrication strategy for gradient tissue engineering. The first criterion is the re-creation of biologically relevant profiles. Stepped transitions commonly formed by sequential layering methods may be appropriate in certain tissue-engineering scenarios, such as the bone–cartilage interface in osteochondral tissue. However, continuous transitions bear greater relevance to most natural systems, enabling improved load transmission and avoiding interfaces that can present mechanical instability or exclude cells. This is linked with the second criterion: the ability to generate complex gradients.

Many strategies, such as those using gravity or buoyancy, are limited to the formation of single, linear gradients. In contrast, natural systems frequently exhibit gradients along different structural axes (e.g., dorsoventral and anteroposterior patterning in the **neural tube** [87]) or in a nonlinear configuration (e.g., radial transitions in the walls of blood vessels [88]). These systems may benefit from the greater design flexibility offered by methods such as 3D printing or the combination of techniques, such as the formation of dual gradients using postmodification of photopatterned hydrogels [82]. Other convergent approaches could be envisaged, such as ice-templating gradients during 3D printing or by forming dual gradients by sequential magnetic field attraction and graded photocrosslinking. A third criterion is the ability to generate dynamic gradients. Natural systems exhibit dynamic changes in morphogen gradient profiles, most notably during different stages of development. This is a major challenge for biomaterial-based strategies, which are generally restricted to simple slow-release morphogen gradients. Cell-secreted enzymes have been used to degrade materials in response to phenotypic changes [89], and similar methods could be used to release morphogen gradients in tune with tissue development and maturation. Alternatively, DeForest and coworkers have demonstrated photoreversible tethering of biomolecules to hydrogels, a method that could be used to extrinsically release morphogen gradients [90].

As well as these technical criteria, it is also important to consider factors that determine academic adoption and translational potential. In this regard, a fourth criterion is the use of accessible equipment. Widespread protocol adoption can be stifled by the specialist knowledge and high costs associated with certain techniques (e.g., bioprinting, microfluidics, two-photon laser scanning). Greater accessibility can be achieved through the use of standard laboratory equipment (e.g., centrifuges), the publication of detailed protocol papers, and the commercialization of dedicated technologies (e.g., gradient makers). A related fifth criterion is system versatility. Many gradient fabrication 'platforms' are demonstrated using a single material, molecule, or tissue; however, techniques that can be more widely applied to different systems will be able to address the needs of a broader user base. In this regard, gradient fabrication should ideally not be constrained by a particular material property (e.g., photoresponsivity, viscosity, magnetism). A sixth criterion, particularly important for translation, is the system reproducibility and robustness. Any scientific method should be reproducible under the reported conditions; however, it is also important that gradient fabrication is not restricted to a narrow parameter space. Ideally, standardized protocols should be used for fabrication with critical-to-quality attributes used to assess the tolerance of the system to process changes. This is linked with the last criterion: the system scalability and throughput. A key process change that should always be assessed is scaling: is the chosen fabrication platform capable of large-scale production of gradient materials? In this regard, systems that are highly automated, rapid, and reproducible will generally enable the high-throughput manufacture required for translational applications.

Concluding Remarks

The tissue engineering community is fully focused on developing methods that can re-create the sophisticated architecture of natural tissues. Here, we have outlined methods for fabricating different gradients present in natural tissues: cellular, compositional, architectural, mechanical, and morphogen. We have presented a new categorization system for the different gradient fabrication strategies based on their underlying rationale: additive manufacturing, component redistribution, controlled phase changes, and postmodification. Many of the studies presented in this Review have focused on osteochondral tissue engineering, but we have also presented examples in which gradient biomaterials are used for *in vitro* bone and cardiac tissue engineering and *in vivo* neural regeneration. These different approaches should be selected and adapted after considering the specific requirements of the target tissue and application. New methodologies are continually being pioneered, and, to this end, we propose a set of ideal criteria for gradient

Outstanding Questions

Can we move from simple 'proof-of-concept' systems to the fabrication of tissue gradients that fully replicate the profile and complexity of gradients found in nature?

Can we produce versatile gradient-casting platforms that use accessible equipment in order to remove barriers to widespread application?

Can we create translational gradient-casting platforms that offer robust and reproducible performance during high-throughput manufacture?

fabrication: the ability to generate biologically-relevant, complex and dynamic gradients, the use of widely accessible equipment, and the system versatility, reproducibility, and robustness (see Outstanding Questions). We hope that this Review will aid and inspire those seeking to develop new gradient biomaterial fabrication methods as well as those applying existing techniques to engineer gradient tissues.

Acknowledgments

C.L. was supported by a Top University Strategic Alliance PhD Scholarship from Taiwan. J.P.K.A. acknowledges support from the Medical Research Council (MRC) (MR/S00551X/1). The authors thank Li Li for the schematic drawing of the Key Figure. L.O. and M.M.S. acknowledge financial support from Engineering and Physical Sciences Research Council (EPSRC) Programme Grant 'Engineering growth factor microenvironments – a new therapeutic paradigm for regenerative medicine' (EP/P001114/1). M.M.S. acknowledges support from a grant from the UK Regenerative Medicine Platform 'Acellular/Smart Materials – 3D Architecture' (MR/R015651/1).

References

1. Sophia Fox, A.J. *et al.* (2009) The basic science of articular cartilage: structure, composition, and function. *Sports Health* 1, 461–468
2. Ren, X. *et al.* (2016) Engineering zonal cartilage through bioprinting collagen type II hydrogel constructs with biomimetic chondrocyte density gradient. *BMC Musculoskelet. Disord.* 17, 301
3. Jadin, K.D. *et al.* (2005) Depth-varying density and organization of chondrocytes in immature and mature bovine articular cartilage assessed by 3D imaging and analysis. *J. Histochem. Cytochem.* 53, 1109–1119
4. Djomehri, S.I. *et al.* (2015) Mineral density volume gradients in normal and diseased human tissues. *PLoS One* 10, E0121611
5. Bergholt, M.S. *et al.* (2016) Raman spectroscopy reveals new insights into the zonal organization of native and tissue-engineered articular cartilage. *ACS Cent. Sci.* 2, 885–895
6. Baron, C. (2012) Using the gradient of human cortical bone properties to determine age-related bone changes via ultrasonic guided waves. *Ultrasound Med. Biol.* 38, 972–981
7. Tobon, C. *et al.* (2013) A three-dimensional human atrial model with fiber orientation: electrograms and arrhythmic activation patterns relationship. *PLoS One* 8, e50883
8. Thomopoulos, S. *et al.* (2003) Variation of biomechanical, structural, and compositional properties along the tendon to bone insertion site. *J. Orthop. Res.* 21, 413–419
9. Zhu, M. *et al.* (2020) Spatial mapping of tissue properties in vivo reveals a 3D stiffness gradient in the mouse limb bud. *Proc. Natl. Acad. Sci. U. S. A.* 117, 4781–4791
10. Zhu, A.J. and Scott, M.P. (2004) Incredible journey: how do developmental signals travel through tissue? *Genes Dev.* 18, 2985–2997
11. Christian, J.L. (2012) Morphogen gradients in development: from form to function. *Wiley Interdiscip. Rev. Dev. Biol.* 1, 3–15
12. Di Luca, A. *et al.* (2015) The osteochondral interface as a gradient tissue: from development to the fabrication of gradient scaffolds for regenerative medicine. *Birth Defects Res. C Embryo Today* 105, 34–52
13. Kronenberg, H.M. (2003) Developmental regulation of the growth plate. *Nature* 423, 332–336
14. Armstrong, J.P.K. and Stevens, M.M. (2019) Emerging technologies for tissue engineering: from gene editing to personalized medicine. *Tissue Eng. Part A* 25, 688–692
15. Armstrong, J.P.K. and Stevens, M.M. (2020) Using remote fields for complex tissue engineering. *Trends Biotechnol.* 38, 254–263
16. Iannucci, L.E. *et al.* (2019) Cellular and chemical gradients to engineer the meniscus-to-bone insertion. *Adv. Healthc. Mater.* 8, e1800806
17. Canadas, R.F. *et al.* (2018) Biochemical Gradients to Generate 3D Heterotypic-Like Tissues with Isotropic and Anisotropic Architectures. *Adv. Funct. Mater.* 28, e1804148
18. Ansari, S. *et al.* (2019) Engineering of gradient osteochondral tissue: from nature to lab. *Acta Biomater.* 87, 41–54
19. Calejo, I. *et al.* (2020) A physiology-inspired multifactorial toolbox in soft-to-hard musculoskeletal interface tissue engineering. *Trends Biotechnol.* 38, 83–98
20. Bracaglia, L.G. *et al.* (2017) 3D printing for the design and fabrication of polymer-based gradient scaffolds. *Acta Biomater.* 56, 3–13
21. Wang, X. *et al.* (2017) Concentration gradient generation methods based on microfluidic systems. *RSC Adv.* 7, 29966–29984
22. Seidi, A. *et al.* (2013) Gradient nanofiber scaffolds for tissue engineering. *J. Nanosci. Nanotechnol.* 13, 4647–4655
23. Niederauer, G.G. *et al.* (2000) Evaluation of multiphase implants for repair of focal osteochondral defects in goats. *Biomaterials* 21, 2561–2574
24. Hong, S.H. *et al.* (2019) Alginate-boronic acid: pH-triggered bioinspired glue for hydrogel assembly. *Adv. Funct. Mater.*, 1908497
25. Guo, J. *et al.* (2017) Multiscale design and synthesis of biomimetic gradient protein/biosilica composites for interfacial tissue engineering. *Biomaterials* 145, 44–55
26. Ko, H. *et al.* (2019) A simple layer-stacking technique to generate biomolecular and mechanical gradients in photocrosslinkable hydrogels. *Biofabrication* 11, 025014
27. Parisi, C. *et al.* (2020) Biomimetic gradient scaffold of collagen-hydroxyapatite for osteochondral regeneration. *J. Tissue Eng.* 11, 204173141989606
28. Levingstone, T.J. *et al.* (2016) Multi-layered collagen-based scaffolds for osteochondral defect repair in rabbits. *Acta Biomater.* 32, 149–160
29. Wei, Z. *et al.* (2017) Dual cross-linked biofunctional and self-healing networks to generate user-defined modular gradient hydrogel constructs. *Adv. Healthc. Mater.* 6, e1700523
30. Ouyang, L. *et al.* (2020) Assembling living building blocks to engineer complex tissues. *Adv. Funct. Mater.*, e1909009
31. Ouyang, L. *et al.* (2019) Void-free 3D bioprinting for in situ endothelialization and microfluidic perfusion. *Adv. Funct. Mater.* 30, e1908349
32. Trachtenberg, J.E. *et al.* (2017) Extrusion-based 3D printing of poly(propylene fumarate) scaffolds with hydroxyapatite gradients. *J. Biomater. Sci. Polym. Ed.* 28, 532–554
33. Bittner, S.M. *et al.* (2019) Fabrication and mechanical characterization of 3D printed vertical uniform and gradient scaffolds for bone and osteochondral tissue engineering. *Acta Biomater.* 90, 37–48
34. Di Luca, A. *et al.* (2016) Influencing chondrogenic differentiation of human mesenchymal stromal cells in scaffolds displaying a structural gradient in pore size. *Acta Biomater.* 36, 210–219
35. Di Luca, A. *et al.* (2016) Gradients in pore size enhance the osteogenic differentiation of human mesenchymal stromal cells in three-dimensional scaffolds. *Sci. Rep.* 6, 22898

36. Smith, B.T. *et al.* (2019) Multimaterial dual gradient three-dimensional printing for osteogenic differentiation and spatial segregation. *Tissue Eng. Part A* 26, 239–252
37. Montazerian, H. *et al.* (2019) Permeability and mechanical properties of gradient porous PDMS scaffolds fabricated by 3D-printed sacrificial templates designed with minimal surfaces. *Acta Biomater.* 96, 149–160
38. Nowicki, M.A. *et al.* (2016) 3D printing of novel osteochondral scaffolds with graded microstructure. *Nanotechnology* 27, 414001
39. Diaz-Gomez, L. *et al.* (2019) Three-dimensional printing of tissue engineering scaffolds with horizontal pore and composition gradients. *Tissue Eng. Part C Methods* 25, 411–420
40. Giachini, P. *et al.* (2020) Additive manufacturing of cellulose-based materials with continuous, multidirectional stiffness gradients. *Sci. Adv.* 6, eaay0929
41. Ayan, B. *et al.* (2020) Aspiration-assisted bioprinting for precise positioning of biologics. *Sci. Adv.* 6, eaaw5111
42. Jeon, O. *et al.* (2019) Individual cell-only bioink and photocurable supporting medium for 3D printing and generation of engineered tissues with complex geometries. *Mater. Horiz.* 6, 1625–1631
43. Lee, A. *et al.* (2019) 3D bioprinting of collagen to rebuild components of the human heart. *Science* 365, 482–487
44. Armstrong, J.P. *et al.* (2016) 3D bioprinting using a templated porous bioink. *Adv. Healthc. Mater.* 5, 1724–1730
45. Moroni, L. *et al.* (2018) Biofabrication strategies for 3D in vitro models and regenerative medicine. *Nat. Rev. Mater.* 3, 21–37
46. Graham, A.D. *et al.* (2017) High-resolution patterned cellular constructs by droplet-based 3D printing. *Sci. Rep.* 7, 7004
47. Hardin, J.O. *et al.* (2015) Microfluidic printheads for multimaterial 3D printing of viscoelastic inks. *Adv. Mater.* 27, 3279–3284
48. Idaszek, J. *et al.* (2019) 3D bioprinting of hydrogel constructs with cell and material gradients for the regeneration of full-thickness chondral defect using a microfluidic printing head. *Biofabrication* 11, 044101
49. Liu, W. *et al.* (2017) Rapid continuous multimaterial extrusion bioprinting. *Adv. Mater.* 29, e1604630
50. Ouyang, L. *et al.* (2016) 3D printing of shear-thinning hyaluronic acid hydrogels with secondary cross-linking. *ACS Biomater. Sci. Eng.* 2, 1743–1751
51. Ouyang, L. *et al.* (2017) A generalizable strategy for the 3D bioprinting of hydrogels from nonviscous photo-crosslinkable inks. *Adv. Mater.* 29, 1604983
52. Zhu, D.Q. *et al.* (2018) Mimicking cartilage tissue zonal organization by engineering tissue-scale gradient hydrogels as 3D cell niche. *Tissue Eng. Part A* 24, 1–10
53. Burdick, J.A. *et al.* (2004) Fabrication of gradient hydrogels using a microfluidics/photopolymerization process. *Langmuir* 20, 5153–5156
54. Orsi, G. *et al.* (2017) A new 3D concentration gradient maker and its application in building hydrogels with a 3D stiffness gradient. *J. Tissue Eng. Regen. Med.* 11, 256–264
55. Hubka, K.M. *et al.* (2019) Perlecan domain I gradients establish stable biomimetic heparin binding growth factor gradients for cell migration in hydrogels. *Acta Biomater.* 97, 385–398
56. Xin, S.J. *et al.* (2019) Creating physicochemical gradients in modular microporous annealed particle hydrogels via a microfluidic method. *Adv. Funct. Mater.* 30, e1907102
57. Costantini, M. *et al.* (2019) 3D-printing of functionally graded porous materials using on-demand reconfigurable microfluidics. *Angew Chem. Int. Ed. Engl.* 58, 7620–7625
58. Zhang, X. *et al.* (2012) Flexible generation of gradient electrospinning nanofibers using a microfluidic assisted approach. *Langmuir* 28, 10026–10032
59. Chow, L.W. *et al.* (2014) Peptide-directed spatial organization of biomolecules in dynamic gradient scaffolds. *Adv. Healthc. Mater.* 3, 1381–1386
60. Kishan, A.P. *et al.* (2017) Fabrication of macromolecular gradients in aligned fiber scaffolds using a combination of in-line blending and air-gap electrospinning. *Acta Biomater.* 56, 118–128
61. Khoo, W. *et al.* (2019) Fracture behavior of multilayer fibrous scaffolds featuring microstructural gradients. *Mater. Des.* 184, 108184
62. Horner, C.B. *et al.* (2019) Spatially regulated multiphenotypic differentiation of stem cells in 3D via engineered mechanical gradient. *ACS Appl. Mater. Interfaces* 11, 45479–45488
63. Forget, A. *et al.* (2020) Facile preparation of tissue engineering scaffolds with pore size gradients using the muesli effect and their application to cell spheroid encapsulation. *J. Biomed. Mater. Res. B Appl. Biomater.* Published online February 12, 2020. https://doi.org/10.1002/jbm.b.34581
64. Harley, B.A. *et al.* (2006) Fabricating tubular scaffolds with a radial pore size gradient by a spinning technique. *Biomaterials* 27, 866–874
65. Oh, S.H. *et al.* (2011) Creating growth factor gradients in three dimensional porous matrix by centrifugation and surface immobilization. *Biomaterials* 32, 8254–8260
66. Li, C. *et al.* (2019) Buoyancy-driven gradients for biomaterial fabrication and tissue engineering. *Adv. Mater.* 31, e1900291
67. He, J. *et al.* (2010) Rapid generation of biologically relevant hydrogels containing long-range chemical gradients. *Adv. Funct. Mater.* 20, 131–137
68. Zwi-Dantsis, L. *et al.* (2020) Remote magnetic nanoparticle manipulation enables the dynamic patterning of cardiac tissues. *Adv. Mater.* 32, e1904598
69. Li, C. *et al.* (2018) Glycosylated superparamagnetic nanoparticle gradients for osteochondral tissue engineering. *Biomaterials* 176, 24–33
70. Xu, G. *et al.* (2020) Electric field-driven building blocks for introducing multiple gradients to hydrogels. *Protein Cell* 11, 267–285
71. Major, L.G. *et al.* (2019) Volume adaptation controls stem cell mechanotransduction. *ACS Appl. Mater. Interfaces* 11, 45520–45530
72. Dou, J. *et al.* (2020) Combination stiffness gradient with chemical stimulation directs glioma cell migration on a microfluidic chip. *Anal. Chem.* 92, 892–898
73. Kim, T.H. *et al.* (2015) Creating stiffness gradient polyvinyl alcohol hydrogel using a simple gradual freezing-thawing method to investigate stem cell differentiation behaviors. *Biomaterials* 40, 51–60
74. Mirab, F. *et al.* (2018) Fabrication and characterization of a starch-based nanocomposite scaffold with highly porous and gradient structure for bone tissue engineering. *Biomed. Phys. Eng. Express* 4, 055021
75. Bai, H. *et al.* (2015) Biomimetic gradient scaffold from ice-templating for self-seeding of cells with capillary effect. *Acta Biomater.* 20, 113–119
76. Pawelec, K.M. *et al.* (2017) Ice-templating of anisotropic structures with high permeability. *Mater. Sci. Eng. C Mater. Biol. Appl.* 76, 628–636
77. Phillips, J.E. *et al.* (2008) Engineering graded tissue interfaces. *Proc. Natl. Acad. Sci. U. S. A.* 105, 12170–12175
78. Liu, W. *et al.* (2014) Nanofiber scaffolds with gradients in mineral content for spatial control of osteogenesis. *ACS Appl. Mater. Interfaces* 6, 2842–2849
79. Gunnewiek, M.K. *et al.* (2015) Creeping proteins in microporous structures: polymer brush-assisted fabrication of 3D gradients for tissue engineering. *Adv. Healthc. Mater.* 4, 1169–1174
80. Xu, Z. *et al.* (2018) Regeneration of cortical tissue from brain injury by implantation of defined molecular gradient of semaphorin 3A. *Biomaterials* 157, 125–135
81. Khetan, S. and Burdick, J.A. (2011) Patterning hydrogels in three dimensions towards controlling cellular interactions. *Soft Matter* 7, 830–838
82. Tong, X.M. *et al.* (2016) Hydrogels with dual gradients of mechanical and biochemical cues for deciphering cell-niche interactions. *ACS Biomater. Sci. Eng.* 2, 845–852
83. Vega, S.L. *et al.* (2018) Combinatorial hydrogels with biochemical gradients for screening 3D cellular microenvironments. *Nat. Commun.* 9, 614
84. Mosiewicz, K.A. *et al.* (2013) In situ cell manipulation through enzymatic hydrogel photopatterning. *Nat. Mater.* 12, 1072–1078
85. Tam, R.Y. *et al.* (2017) Engineering cellular microenvironments with photo- and enzymatically responsive hydrogels: toward

biomimetic 3D cell culture models. *Acc. Chem. Res.* 50, 703–713

86. Fisher, S.A. *et al.* (2018) Photo-immobilized EGF chemical gradients differentially impact breast cancer cell invasion and drug response in defined 3D hydrogels. *Biomaterials* 178, 751–766
87. Ulloa, F. and Briscoe, J. (2007) Morphogens and the control of cell proliferation and patterning in the spinal cord. *Cell Cycle* 6, 2640–2649
88. Galliger, Z. *et al.* (2019) 3D bioprinting for lungs and hollow organs. *Transl. Res.* 211, 19–34
89. Parmar, P.A. *et al.* (2016) Temporally degradable collagen-mimetic hydrogels tuned to chondrogenesis of human mesenchymal stem cells. *Biomaterials* 99, 56–71
90. Deforest, C.A. and Tirrell, D.A. (2015) A photoreversible protein-patterning approach for guiding stem cell fate in three-dimensional gels. *Nat. Mater.* 14, 523–531